Nanoparticles Hot Paper

How to cite:
International Edition: doi.org/10.1002/anie.202210140
German Edition: doi.org/10.1002/ange.202210140

Photo-Induced Microfluidic Production of Ultrasmall Glyco Gold Nanoparticles

*Patricia Perez Schmidt, Katiuscia Pagano, Cristina Lenardi, Marta Penconi, Ruth Mateu Ferrando, Claudio Evangelisti, Luigi Lay, Laura Ragona, Marcello Marelli, and Laura Polito**

Abstract: Ultra-small gold nanoparticles (UAuNPs) are extremely interesting for applications in nanomedicine thanks to their good stability, biocompatibility, long circulation time and efficient clearance pathways. UAuNPs engineered with glycans (Glyco-UAuNPs) emerged as excellent platforms for many applications since the multiple copies of glycans can mimic the multivalent effect of glycoside clusters. Herein, we unravel a straightforward photo-induced synthesis of Glyco-UAuNPs based on a reliable and robust microfluidic approach. The synthesis occurs at room temperature avoiding the use of any further chemical reductant, templating agents or co-solvents. Exploiting ^{1}H NMR spectroscopy, we showed that the amount of thiol-ligand exposed on the UAuNPs is linearly correlated to the ligand concentration in the initial mixture. The results pave the way towards the development of a programmable synthetic approach, enabling an accurate design of the engineered UAuNPs or smart hybrid nanosystems.

[*] P. Perez Schmidt, Dr. M. Penconi, Dr. M. Marelli, Dr. L. Polito
Istituto di Scienze e Tecnologie Chimiche "Giulio Natta", SCITEC-CNR, Via G. Fantoli 16/15, 20138 Milano (Italy)
E-mail: laura.polito@scitec.cnr.it

Dr. K. Pagano, Dr. L. Ragona
Istituto di Scienze e Tecnologie Chimiche "Giulio Natta", SCITEC-CNR, Via A. Corti 12, 20131 Milano (Italy)

Prof. Dr. C. Lenardi
Interdisciplinary Centre for Nanostructured Materials and Interfaces (CIMAINA), Department of Physics, Università degli Studi di Milano, Via Celoria 16, 20133 Milano Italy
and
Fondazione UNIMI, Viale Ortles 22/4, 20139 Milano (Italy)

R. M. Ferrando, Prof. Dr. L. Lay
Department of Chemistry, Università degli Studi di Milano via C. Golgi 19 20133 Milano (Italy)

Dr. C. Evangelisti
Institute of Chemistry of Organo Metallic Compounds, ICCOM-CNR, Via G. Moruzzi 1, 56124 Pisa (Italy)

Ultrasmall gold nanoparticles (UAuNPs) are characterized by a core diameter lower than 5 nm, tunable optical properties, ease of surface chemical modification, luminescence, prolonged stability in different media and high biocompatibility.[1,2] In nanomedicine, UAuNPs have several significant advantages with respect to bigger nanoparticles, such as longer circulation time, improved biodistribution, better tissue penetration and efficient clearance pathways. The use of UAuNPs in biomedical applications has been increasingly explored over the past decade both in diagnosis, thanks to their luminescence emission, and in therapy. Specifically, UAuNPs showed excellent penetration ability in tumor tissues,[3] triggering an effective enhancement as ultrasound contrast agents[4] or during radiation therapy,[5,6] together with an excellent antibacterial action.[7] Thanks to the strong soft-soft interaction between Au surface and sulfur, UAuNPs can be easily functionalized with molecules bearing thiol groups. Exploiting this strategy, many examples of glycosylated UAuNPs have been reported in the last years.[8–12] Indeed carbohydrates, ubiquitous in all organisms, play a pivotal role in promoting and driving many biological events. Carbohydrates establish weak interactions with their receptors and nature finely modulates carbohydrate-mediated recognition events by clustering glycans into multivalent systems (the so called "cluster glycoside effect").[13,14] Taking inspiration from living cells, many different systems carrying multiple copies of glycans have been designed to mimic the multivalent effect of glycoside clusters.[15,16] In this frame, UAuNPs decorated with glycans showed exciting results, representing a great opportunity for next generation therapeutics.[10,17] However, to fulfill the ambitious potentiality of these engineered UAuNPs, robust protocols for their synthesis, functionalization and characterization, are still needed and highly desirable.

Up to now, the most common strategy employed to produce ultrasmall AuNPs is based on the synthesis developed in 1994 by Brust and Schriffin and the following modifications.[18,19] The synthetic procedure is based on a biphasic reduction reaction using tetraoctylammonium bromide (TOAB) as phase transfer reagent and sodium borohydride ($NaBH_4$) as strong reducing agent. To immediately stabilize the small AuNPs, strong capping agents (i.e. alkanethiol) or toxic templating agents (i.e. hexadecyl(trimethyl)ammonium bromide, CTAB) are added to the mixture. To introduce the desired functionalization

on the NP surface, the capped-AuNPs must undergo multi-steps approach such as ligand exchange or phase transfer from organic to aqueous solutions, resulting in poor size distribution and low yields.[19,20] Exploiting this approach, Penadès and collaborators developed a direct synthesis of glyco-gold nanoparticles in 1–10 nm diameter range, using sodium borohydride and thiol-derivatives.[11] With their seminal work, authors were able to conjugate different thio-ligands, confirming that the ratio used in the reaction mixture was maintained on the nanoparticle surface. Despite the success of this strategy, new synthetic one-pot approaches to produce UAuNPs avoiding the use of sodium borohydride or template agents are highly demanded. Recently, new protocols have been introduced, but still requiring high temperatures and/or long reaction times.[4,7,21]

In the last years, microfluidic reactors have emerged as outstanding tools for synthesizing a wide range of nanoparticles allowing for a fine control over particle size, morphology and reproducibility.[21–25] In our previous works[26,27] we showed that in-flow chemistry can represent a robust alternative platform for the production of customized nanoparticles. The technique ensures superior heat- and mass-transfer rates, allowing the synthesis of both isotropic and anisotropic NPs[27] with size larger than 10 nm and complex hybrid nanomaterials.[26] These protocols cannot be easily adapted to UAuNPs production as they would require a strong reductive agent (to promote a fast nucleation step) and the presence of a capping agent (to stop the growth stage). For example, Gavriilidis and collaborators[21] accomplished the production of citrate-capped UAuNP enhancing the nucleation rate by means of a controlled flow through capillaries but still employing elevated temperature.

Herein we report a robust and reliable protocol to synthesize one-pot Glyco-UAuNPs. It is based on a photo-induced microfluidic approach carried out at room temperature over two hours of reaction and without the addition of templating or reducing agents (Figure 1). The procedure is highly reproducible, and allows a straightforward purification of the functionalized UAuNPs, together with the recovery of the unreacted precious ligands, that can be used in further synthesis. To achieve the in-flow synthesis of AuNPs smaller than 5 nm, we coupled the advantages of the microfluidic protocol with the ability of UV-light to reduce metal atoms, at room temperature.[28–31] The photochemical approach promotes the decomposition of the solvent (water or alcohol) by UV-light and the formation of hydroxyl radicals and solvated electrons that act as the efficient reducing species. The protocol has been tested on a set of glyco-derivatives bearing an amphiphilic or an aliphatic linker containing a thiol moiety, which ensures the effective functionalization of the metal surface (Supporting Information, Table S1–S3). The results showed that the approach is effective independently from the nature of the glycans, highlighting the wide applicability of the method to different ligands bearing an available thiol-moiety.

In our general and optimized procedure (see Supporting Information) mannose-derivative 1-Man (12 mg) was added to 4.5 mL of a degassed solution of water containing 10 % v/v of ethanol, followed by the addition of 0.5 mL of a 10 mM $HAuCl_4$ in water. Ligand 1-Man is a mixture of 61 % mannose glycosylated to the amphiphilic linker (EG_6C_{11}-SH) and 39 % of the free HO-EG_6C_{11}-SH, as assessed by quantitative NMR analysis (ERETIC2, see Supporting Information). The mixture was infused by a peristaltic pump at 0.25 mL min^{-1} through a fluorinated ethylene propylene (FEP) tube (0.762 mm ID, 5 m length) coiled around a water-cooled UV lamp (Figure 1). The circulating mixture was exposed to the UV-light for 2 hours, monitoring the reaction progress by UV/Vis spectroscopy (Supporting Information, Figure S1). After that time, the engineered UAuNPs were collected in a conical tube and purified by means of centrifugation (6 minutes, 6000 rpm), affording stable and monodisperse mannosylated gold nanoparticles (1-Man-UAuNPs) with a yield of 71 %, as deter-

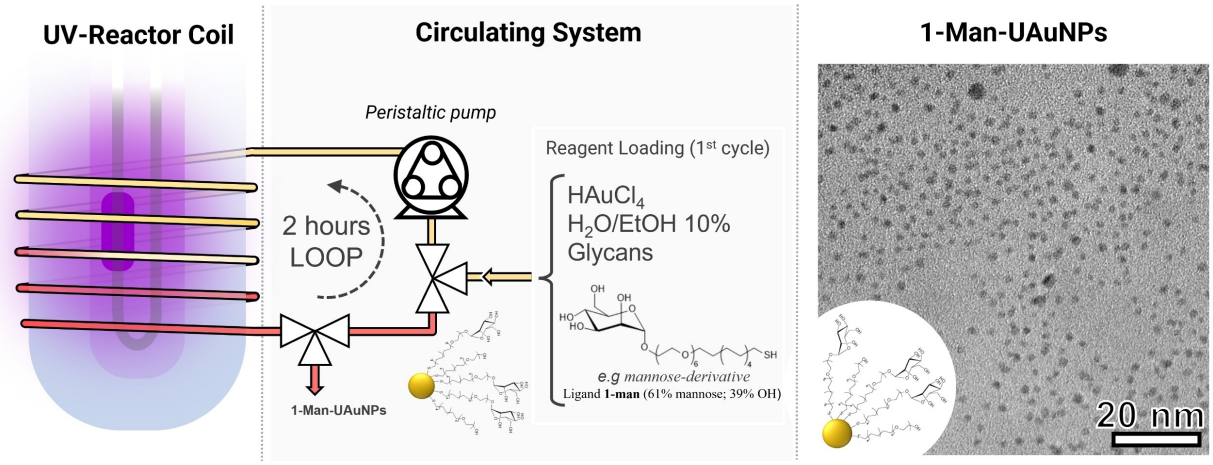

Figure 1. Synthesis of mannose-gold nanoparticles (left) and TEM micrograph of Mannose ultrasmall gold nanoparticles (right).

mined by analyzing the Au content by Inductively Coupled Plasma-Optical Emission Spectrometry (ICP-OES). An average core diameter of 2.3 nm was measured by means of Transmission Electron Microscopy, TEM (Figure 1 and Supporting Information Table S4).

The complete reduction of gold was proven by X-ray photoelectron spectroscopy (XPS) that showed a good match with the metal reference, without evidence of Au^+ species, while the peaks appear slightly larger due to the nanosized nature of the UAuNPs (Supporting Information, Figure S5). XPS also confirms the presence of S coordinated with Au species, as attested by the position of S 2p (162.5 eV)[32] and the C–C and C–O species are attributable to the functionalization of the UAuNP surface and not to any environmental contamination of sample surface.

In Figure 2 we report and compare the ^{1}H NMR spectra recorded on 1-Man and 1-Man-UAuNPs. The strong broadening of the proton resonances in the direct surroundings of thiol groups of the ligand (2.626 and 2.484 ppm for Hβ of mannose-EG_6C_{11} and OH-EG_6C_{11}, respectively) confirm the binding of ligand 1-Man to the gold nanoparticle (Figure 2, lower panel).[33] The quantification of the bound mannose-derivative on each ultrasmall gold nanoparticle was achieved by exploiting a quantitative ^{1}H NMR study (ERETIC2, Supporting Information). The amount of mannose on the UAuNPs was estimated to 7.85 ± 0.35 mM by integrating the resonances at 4.806 (anomeric proton) and 3.876 (proton on C6 of the saccharide chain) ppm (Figure 2), corresponding to an estimated glycan density of 469 mannose-derivative molecules per NP (see Supporting Information for details on the calculation).

Quantitative analysis performed in parallel (see Supporting Information) on ligand 1-Man, not-purified 1-Man-UAuNPs, purified 1-Man-UAuNPs and related supernatant showed that an almost total recovery of the unreacted ligand 1-Man was possible. In fact, the absence of any templating or reducing agent in our protocol, with respect to the conventional $NaBH_4$ based procedures, allows the recovery of unbounded ligand as a pure compound without any further by-products, as determined by ^{1}H NMR. Altogether, the results highlight the high value and the significance of the proposed protocol in terms of overall UAuNP yields, ligand regaining and its potential recyclability. 1-Man-UAuNPs were further characterized by diffusion-ordered NMR spectroscopy (DOSY) to derive information on the hydrodynamic radius of the functionalized UAuNP. DOSY experiment (Supporting Information, Figure S7) provided a translational diffusion coefficient of $(5.5 \pm 0.1) \times 10^{-11}$ $m^2 s^{-1}$, that can be directly related to an effective hydrodynamic radius by Stokes–Einstein equation.[34–36] Assuming a spherical geometry and using the diffusion measured for dioxane molecule, added to the sample as internal standard, a hydrodynamic radius of 3.3 ± 0.1 nm was derived. The hydrodynamic diameter (6.6 nm), estimated by NMR, is higher than the one measured by TEM (2.3 nm), reporting the size of the NP core. NMR diffusion data thus allowed to estimate the effective increase of size following UAuNP functionalization.

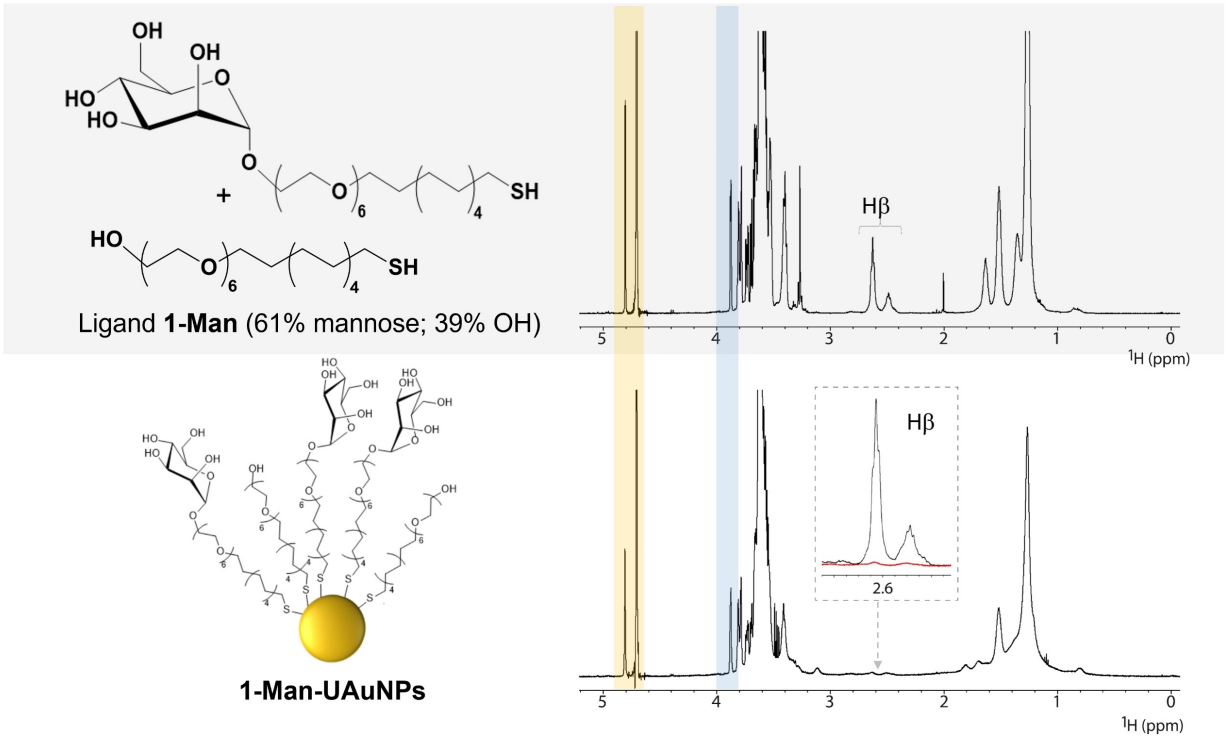

Figure 2. ^{1}H NMR of ligand **1-Man** (upper) and **1-Man-UAuNPs** (lower). A magnification of Hβ region is reported in the inset for 1-Man (black) and 1-Man-UAuNPs (red).

In light of newly synthesized 1-Man-UAuNPs relevance in biomedical imaging, their fluorescence behavior was investigated.[37]

1-Man-UAuNPs resulted to be luminescent in the near infrared (NIR) region. In particular, 1-Man-UAuNPs dispersed in water displayed NIR emission peaked at 820 nm with quantum yield of 1.8 % and excitation maximum around 310 nm (Supporting Information, Figure S8), in agreement with the photoluminescence reported for gold nanoparticles of similar size.[1,4,38]

The reliability of the in-flow protocol has been established by synthesizing a set of Glyco-UAuNPs functionalized with different glycans bearing the same amphiphilic thiol-spacer (EC_6C_{11}-SH) and measuring by ^{1}H NMR both the initial amount and the final loading of each ligand on UAuNPs (Figure 3).

In addition to 1-Man, the glyco-derivatives bearing glucose (2-Glc) at two different initial concentrations, lactose (3-Lac) at three different initial concentrations, and a 1:1 ratio mixture of 2-Glc/3-Lac were employed to test the protocol. The use of the amphiphilic linker at the anomeric position of the three glycans ensured a highly stable colloidal solution and the protocol afforded functionalized UAuNPs with high reproducibility in terms of yield and size (Supporting Information, Table S4 and Table S5). ^{1}H-quantitative NMR analysis has been successfully used to determine the loading of the glycans in homo-functionalized UAuNPs (1-Man-UAuNPs, 2-Glc-UAuNPs, 2-Glc-UAuNPs*, 3-Lac-UAuNPs, 3-Lac-UAuNPs* and 3-Lac-UAuNPs°) as in hetero-functionalized NPs (4-Glc/Lac-UAuNPs*). Altogether, the NMR results demonstrate that, in the explored concentration range, the final loading is independent from the nature of the glycans and is linearly correlated to the initial HS-ligand concentration (Figure 3). To further confirm and bolster this behavior, three different glyco ligands (2-Glc*, 3-Lac* and 4-Glc/Lac*) were employed at the same initial amount (11.6 µmol) affording a comparable amount of ligand on UAuNP surface as shown in Figure 3. The figure obtained from data fitting can be easily employed to shape the ligand density on the NPs with high precision, thus guiding the design of even complex surface-functionalized UAuNPs. Notably, in the case of 4-Glc/Lac-UAuNPs*, the initial µmol lactose/glucose ratio, 1.9, calculated on the basis of the effective carbohydrate fraction present in each ligand (Figure 3, upper panel) was retained on the UAuNP surface (1.8) as determined by ^{1}H quantitative NMR (Supporting Information, Table S7).[11] In order to asses and evaluate the stability of these UAuNPs over time, 2-Glc-UAuNPs were analyzed by UV/Vis and TEM after being dispersed in different media (PBS and Roswell Park Memorial Institute, RPMI) and in presence of reduced glutathione, GSH. Data indicate that no changes occurred in terms of aggregation or core modification (Figure S9 and S10). Glyco-UAuNPs synthesized under the new proposed protocol can be considered stable over the time of observation in water (up to 9 months) and in PBS, RPMI, GHS (1 week). The presence of GSH, selected to mimic biogenic thiols, does not induce ligand exchange over

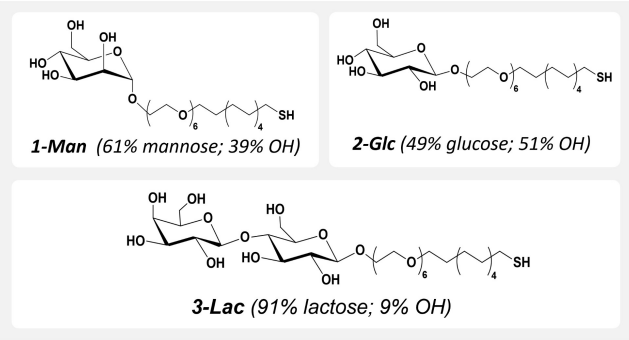

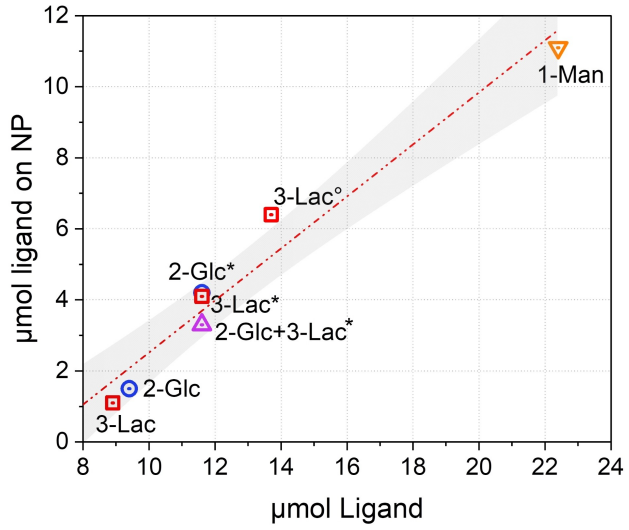

Glyco-UAuNPs	HS-Ligand	µmol HS-Ligand	µmol HS-Ligand on UAuNPs
1-Man-UAuNPs	1-Man	22.4	11.1
2-Glc-UAuNPs	2-Glc	9.4	1.5
2-Glc-UAuNPs*	2-Glc*	**11.6**	4.2
3-Lac-UAuNPs	3-Lac	8.9	1.1
3-Lac-UAuNPs*	3-Lac*	**11.6**	4.1
3-Lac-UAuNPs°	3-Lac°	13.7	6.4
4-Glc/Lac-UAuNPs*	2-Glc + 3-Lac (1:1)*	**11.6**	3.3

Figure 3. Upper panel: Structures of the ligands 1-Man, 2-Glc, 3-Lac; Middle panel: Linear correlation between µmol of HS-ligand present in the initial mixture respect to the µmol of HS-ligand displayed on the nanoparticle surface; Lower panel: summary of data represented in the graph. *Samples with equal initial HS-Ligand amount (11.6 µmol), °3-Lac-UAuNPs sample with initial HS-Ligand amount of 13.7 µmol.

nanoparticle surface, as determined by ^{1}H NMR data on supernatant (Figure S11).

To further generalize the application of the proposed synthetic protocol, we evaluated the use of short aliphatic chains and highly hydrophilic linkers. We successfully tested glycan derivatives (Supporting Information, Table S2) bearing short aliphatic C_2 or C_3 chains, namely 5-Man, 6-Glc, 7-Lac or long poly(ethylene glycol) chains (HS-PEG, MW 5 kDa), namely 8-PEG and 9-GalPEG (see Supporting Information, Table S3). Short aliphatic linkers did not hamper the effectiveness of the UAuNPs formation (Figure S1), however a decrease of water dispersibility was

observed for UAuNPs 5–7, making the colloidal solutions of these UAuNPs less stable with respect to those obtained from amphiphilic linkers. The ligand density on Glyco-UAuNPs 5–7 could not be determined by ^{1}H NMR as the proximity of the ligand to the gold core induced a strong broadening of all the ligand resonances hampering a quantitative analysis (Figure S6). On the other hand, we selected thiol-PEG_{5000} linkers as they are broadly used to cap AuNP surface to minimize nonspecific adsorption of proteins onto nanoparticle surfaces, reducing AuNP uptake by macrophages in *in vivo* applications.[39] Both thio-PEG_{5000}-NH_2 (8-PEG) and thio-PEG_{5000}-Galactose (9-GalPEG) afforded stable PEG_{5000}-UAuNPs (Figure S1), highlighting the versatility and customization of the present protocol. The ligand density on 9-GalPEG-UAuNPs could be determined exploiting ERETIC ^{1}H NMR method (see Supporting Information and Table S7).

In summary, we developed an optimized, robust and reliable microfluidic protocol to produce glyco-functionalized UAuNPs. We synergically coupled the in-flow advantages with a photo-induced reduction promoted by a UV-lamp in order to produce sub-3 nm AuNPs at room temperature and in two hours of reaction. We avoided the use of strong reducing agents, toxic templating compounds or co-solvents, exploiting greener conditions. A simple purification step, based on a centrifugation, allowed the collection of the desired glyco-UAuNPs and the almost total recovery of the not reacted thiol-derivatives. The glycan loading on AuNP surface was estimated by quantitative NMR measurements, demonstrating the fine ability of the proposed protocol to shape UAuNP ligand density. Furthermore, we demonstrated that the protocol can be successfully extended to different glycans bearing both aliphatic and long PEG thiol-linkers. We envisage that the developed strategy paves the way to a generalized protocol for the production, even in large scale, of functionalized UAuNPs through a highly reproducible approach that can be further automatized and customized.

Acknowledgements

This project has received funding from the European Union's Horizon 2020 research and innovation programme under the Marie Skłodowska-Curie grant agreement No 814236. L.P. and L.L. acknowledge COST Action CA18103: INNOGLY: INNOvation with GLYcans, new frontiers from synthesis to new biological targets. K.P. and L.R. acknowledge Fondazione Antonio De Marco support. P.P.S. and L.P. thanks Africa G. Barrientos, John Porter and Midatech Pharma PLC (Bilbao, Spain) for generous gift of ligands 1–7.

Conflict of Interest

The authors declare no conflict of interest.

Data Availability Statement

The data that support the findings of this study are available in the Supporting Information of this article.

Keywords: Carbohydrates · Glyco Gold Nanoparticles · Microfluidics · Photoreduction · Ultrasmall Gold Nanoparticles

[1] L. Gong, K. He, J. Liu, *Angew. Chem. Int. Ed.* **2021**, *60*, 5739–5743; *Angew. Chem.* **2021**, *133*, 5803–5807.
[2] S. E. Crawford, M. J. Hartmann, J. E. Millstone, *Acc. Chem. Res.* **2019**, *52*, 695–703.
[3] M. Fan, Y. Han, S. Gao, H. Yan, L. Cao, Z. Li, X. J. Liang, J. Zhang, *Theranostics* **2020**, *10*, 494–4957.
[4] Y. Tan, M. Chen, H. Chen, J. Wu, J. Liu, *Angew. Chem. Int. Ed.* **2021**, *60*, 11713–11717; *Angew. Chem.* **2021**, *133*, 11819–11823.
[5] A. Kefayat, F. Ghahremani, H. Motaghi, A. Amouheidari, *Nanomedicine* **2019**, *16*, 173–184.
[6] X. D. Zhang, Z. Luo, J. Chen, S. Song, X. Yuan, X. Shen, H. Wang, Y. Sun, K. Gao, L. Zhang, S. Fan, D. T. Leong, M. Guo, J. Xie, *Sci. Rep.* **2015**, *5*, 8669.
[7] Y. Xie, J. Yang, J. Zhang, W. Zheng, X. Jiang, *Angew. Chem. Int. Ed.* **2020**, *59*, 23471–23475; *Angew. Chem.* **2020**, *132*, 23677–23681.
[8] D. Budhadev, E. Poole, I. Nehlmeier, Y. Liu, J. Hooper, E. Kalverda, U. S. Akshath, N. Hondow, W. B. Turnbull, S. Pöhlmann, Y. Guo, D. Zhou, *J. Am. Chem. Soc.* **2020**, *142*, 18022–18034.
[9] C. Ghosh, S. Varela-Aramburu, H. E. Eldesouky, S. Salehi Hossainy, M. N. Seleem, T. Aebischer, P. H. Seeberger, *Adv. Ther.* **2021**, *4*, 2000293.
[10] M. Anderluh, F. Berti, A. Bzducha-Wróbel, F. Chiodo, C. Colombo, F. Compostella, K. Durlik, X. Ferhati, R. Holmdahl, D. Jovanovic, W. Kaca, L. Lay, M. Marinovic-Cincovic, M. Marradi, M. Ozil, L. Polito, J. J. Reina, C. A. Reis, R. Sackstein, A. Silipo, U. Švajger, O. Vaněk, F. Yamamoto, B. Richichi, S. J. van Vliet, *FEBS J.* **2022**, *289*, 4251–4303.
[11] M. Marradi, F. Chiodo, I. García, S. Penadés, *Chem. Soc. Rev.* **2013**, *42*, 4728–4745.
[12] F. Compostella, O. Pitirollo, A. Silvestri, L. Polito, *Beilstein J. Org. Chem.* **2017**, *13*, 1008–1021.
[13] F. Peri, *Chem. Soc. Rev.* **2013**, *42*, 4543–4556.
[14] A. Bernardi, J. Jiménez-Barbero, A. Casnati, C. De Castro, T. Darbre, F. Fieschi, J. Finne, H. Funken, K. E. Jaeger, M. Lahmann, T. K. Lindhorst, M. Marradi, P. Messner, A. Molinaro, P. V. Murphy, C. Nativi, S. Oscarson, S. Penadés, F. Peri, R. J. Pieters, O. Renaudet, J. L. Reymond, B. Richichi, J. Rojo, F. Sansone, C. Schäffer, W. B. Turnbull, T. Velasco-Torrijos, S. Vidal, S. Vincent, T. Wennekes, H. Zuilhof, A. Imberty, *Chem. Soc. Rev.* **2013**, *42*, 4709–4727.
[15] A. K. Adak, H.-J. Lin, C.-C. Lin, *Org. Biomol. Chem.* **2014**, *12*, 5563–73.
[16] R. Sunasee, R. Narain, *Macromol. Biosci.* **2013**, *13*, 9–27.
[17] R. Mateu Ferrando, L. Lay, L. Polito, *Drug Discovery Today Technol.* **2020**, *38*, 57–67.
[18] M. Brust, M. Walker, D. Bethell, D. J. Schiffrin, R. Whyman, *J. Chem. Soc. Chem. Commun.* **1994**, 801–802.
[19] P. Zhao, N. Li, D. Astruc, *Coord. Chem. Rev.* **2013**, *257*, 638–665.
[20] T. Tu, W. Zhou, M. Wang, X. Guo, L. Li, M. A. Cohen Stuart, J. Wang, *Ind. Eng. Chem. Res.* **2020**, *59*, 11080–11086.
[21] H. Huang, H. du Toit, M. O. Besenhard, S. Ben-Jaber, P. Dobson, I. Parkin, A. Gavriilidis, *Chem. Eng. Sci.* **2018**, *189*, 422–430.

[22] E. J. Roberts, S. E. Habas, L. Wang, D. A. Ruddy, E. A. White, F. G. Baddour, M. B. Griffin, J. A. Schaidle, N. Malmstadt, R. L. Brutchey, *ACS Sustainable Chem. Eng.* **2017**, *5*, 632–639.
[23] L. Panariello, S. Damilos, H. Du Toit, G. Wu, A. N. P. Radhakrishnan, I. P. Parkin, A. Gavriilidis, *React. Chem. Eng.* **2020**, *5*, 663–676.
[24] G. Tofighi, H. Lichtenberg, J. Pesek, T. L. Sheppard, W. Wang, L. Schöttner, G. Rinke, R. Dittmeyer, J. D. Grunwaldt, *React. Chem. Eng.* **2017**, *2*, 876–884.
[25] J. Nette, P. D. Howes, A. J. DeMello, *Adv. Mater. Technol.* **2020**, *5*, 2000060.
[26] M. Marelli, F. Bossola, G. Spinetti, E. Sangalli, V. D. Santo, R. Psaro, L. Polito, *ACS Appl. Mater. Interfaces* **2020**, *12*, 38522–38529.
[27] A. Silvestri, L. Lay, R. Psaro, L. Polito, C. Evangelisti, *Chem. Eur. J.* **2017**, *23*, 9732–9735.
[28] Y. Shiraishi, H. Tanaka, H. Sakamoto, S. Ichikawa, T. Hirai, *RSC Adv.* **2017**, *7*, 6187–6192.
[29] M. Harada, S. Kizaki, *Cryst. Growth Des.* **2016**, *16*, 1200–1212.
[30] H. Du Toit, T. J. Macdonald, H. Huang, I. P. Parkin, A. Gavriilidis, *RSC Adv.* **2017**, *7*, 9632–9638.
[31] M. Harada, K. Saijo, N. Sakamoto, *Colloids Surf. A* **2009**, *349*, 176–188.
[32] Y. Mikhlin, M. Likhatski, Y. Tomashevich, A. Romanchenko, S. Erenburg, S. Trubina, *J. Electron Spectrosc. Relat. Phenom.* **2010**, *177*, 24–29.
[33] S. B. van der Meer, T. Seiler, C. Buchmann, G. Partalidou, S. Boden, K. Loza, M. Heggen, J. Linders, O. Prymak, C. L. P. Oliveira, L. Hartmann, M. Epple, *Chem. Eur. J.* **2021**, *27*, 1451–1464.
[34] D. K. Wilkins, S. B. Grimshaw, V. Receveur, C. M. Dobson, J. A. Jones, L. J. Smith, *Biochemistry* **1999**, *38*, 16424–16431.
[35] L. Ragona, O. Gasymov, A. J. Guliyeva, R. B. Aslanov, S. Zanzoni, C. Botta, H. Molinari, *Biochim. Biophys. Acta Proteins Proteomics* **2018**, *1866*, 661–667.
[36] K. Pagano, L. Carminati, S. Tomaselli, H. Molinari, G. Taraboletti, L. Ragona, *ChemBioChem* **2021**, *22*, 160–169.
[37] Y. Huang, L. Fuksman, J. Zheng, *Dalton Trans.* **2018**, *47*, 6267–6273.
[38] X. Tu, W. Chen, X. Guo, *Nanotechnology* **2011**, *22*, 095701.
[39] L. Sanchez, Y. Yi, Y. Yu, *Nanoscale* **2017**, *9*, 288–297.

Manuscript received: July 11, 2022
Accepted manuscript online: November 2, 2022
Version of record online: ■■, ■■

Communications

Nanoparticles

P. Perez Schmidt, K. Pagano, C. Lenardi, M. Penconi, R. M. Ferrando, C. Evangelisti, L. Lay, L. Ragona, M. Marelli, L. Polito* _____ **e202210140**

Photo-Induced Microfluidic Production of Ultrasmall Glyco Gold Nanoparticles

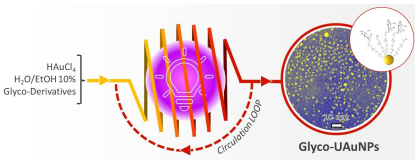

We propose a robust, fast and green synthetic route to produce ultrasmall glyco gold nanoparticles (glyco-UAuNP) by an innovative photo-induced microfluidic approach. The absence of templating and reducing agents allows a simple product purification and the recovery of the unbound thiol-ligand. We successfully built a set of glyco-UAuNP library, testing different combinations of linker/sugar and shaping the UAuNP glyco-ligand density.